Scientific Research Publishing

American Journal of Plant Sciences, 2019, 10, 1325-1349
http://www.scirp.org/journal/ajps
ISSN Online: 2158-2750
ISSN Print: 2158-2742

Difference in Nitrogen Starvation-Inducible Expression Patterns among Phylogenetically Diverse Ammonium Transporter Genes in the Red Seaweed *Pyropia yezoensis*

Chengze Li[1], Inori Ariga[1], Koji Mikami[2*]

[1]Graduate School of Fisheries Sciences, Hokkaido University, Hakodate, Japan
[2]Faculty of Fisheries Sciences, Hokkaido University, Hakodate, Japan
Email: *komikami@fish.hokudai.ac.jp

How to cite this paper: Li, C.Z., Ariga, I. and Mikami, K. (2019) Difference in Nitrogen Starvation-Inducible Expression Patterns among Phylogenetically Diverse Ammonium Transporter Genes in the Red Seaweed *Pyropia yezoensis*. *American Journal of Plant Sciences*, **10**, 1325-1349.
https://doi.org/10.4236/ajps.2019.108096

Received: July 4, 2019
Accepted: August 20, 2019
Published: August 23, 2019

Abstract

Nitrogen deficiency induces senescence and the expression of genes encoding ammonium transporters (AMTs) in terrestrial plants where the AMT family is subdivided into AMT1 and AMT2 subfamilies. Nitrogen starvation in the red seaweed *Pyropia yezoensis* causes senescence-like discoloration. In this study, we identified five genes in *P. yezoensis* encoding AMT domain-containing proteins, which were phylogenetically categorized into the AMT1 subfamily. We also found a gene encoding a Rhesus protein (Rh) that was related to, but diverged from, AMTs. Moreover, our phylogenetic analysis showed that AMT domain-containing proteins from micro- and macro-algae belonged to either the AMT1 or Rh subfamily, indicating the absence of AMT2 in algae. Gene expression analyses revealed the presence of gametophyte- and sporophyte-specific AMT1 genes that were up-regulated transiently and continually, respectively, under nitrogen-deficient conditions. In addition, up-regulated sporophyte-specific gene expression was suppressed when nitrogen was re-supplied. Accordingly, an expansion of the ancient AMT gene has produced AMT1 functional variants differing in temporal and nitrogen starvation-inducible expression patterns during the life cycle of *P. yezoensis*. These findings help elucidate the unique nutrition starvation responses involving functionally diverse AMT1 and Rh subfamilies in red seaweed.

Keywords

Ammonium Transporter, Discoloration, Nitrogen, *Pyropia yezoensis*

1. Introduction

Ammonium (NH_4^+) is a major nitrogen source for higher plants and algae [1]

[2] [3] and is used in the biosynthesis of nitrogen-containing compounds such as amino acids and nucleic acids [4] [5]. The influx of extracellular NH_4^+ into cells is mediated by ammonium transporters (AMTs) [6]. In plants, AMTs are encoded by a multigene family comprising the AMT1 and AMT2 subfamilies [2] [7]. AMT1s are responsible for high-affinity NH_4^+ transport in rice (*Oryza sativa*), wheat (*Triticum aestivum*) and many other plant species [5] [7] [8] [9] [10]. Genes encoding AMT1s show different expression patterns. For instance, in *Arabidopsis thaliana*, *AtAMT*1; 1 is expressed in the roots and leaves [4] and the expression of *AtAMT*1; 2/1; 3 and *AtAMT*1; 5 is mostly restricted to roots [11], while *AMT*1; 4 shows pollen-specific expression [12]. In addition, *AtAMT*1; 1 and *AtAMT*1; 3 are induced by nitrogen starvation, whereas *AtAMT*1; 2 expression is insensitive to nitrogen deficiency [13]. A recent study showed that the protein encoded by *AtAMT*2; 1 transfers NH_4^+ from roots to shoots [14], but the physiological functions of AMT2s are less understood than those of AMT1s.

In the red seaweed *Pyropia yezoensis*, nitrogen limitation induces severe discoloration in the gametophytic thallus due to a 20% - 50% reduction of the pigment content [15]. Discoloration in thallus decreases its quality as a food [16] [17]. This discoloration can be rescued by increasing the nitrogen concentration in the medium [15] [16]. Of the various nitrogen sources, NH_4^+ is preferentially used over NO_3^-, urea, and other organic nitrogen sources in *P. yezoensis* [15] [16], suggesting the importance of AMTs for nitrogen homeostasis in this species. Genomic and transcriptomic analyses have identified several AMT genes in algae, including the green algae *Chlamydomonas reinhardtii* [3] [18] and *Volvox carteri* [19], the red algae *Galdieria sulphuraria* [20] and *Porphyra umbilicalis* [21], and the diatom *Cylindrotheca fusiformis* [22]. Of these, expression of one of the AMT genes in *Po. umbilicalis* and *CfAMT*1 from *Cylindrotheca fusiformis* was up-regulated under low-nitrogen conditions [22] [23]. In contrast, AMT genes in *P. yezoensis* are currently restricted to *PyAMT*1, whose expression is also induced under nitrogen-deficient conditions.

The *P. yezoensis* life cycle consists of gametophyte and sporophyte generations [24] [25]. The nitrate transporter gene *PyNRT*2 shows gametophyte-specific expression [26]. Among three urea transporter genes (*PyDUR*3.1, *PyDUR*3.2, and *PyDUR*3.3) in *P. yezoensis*, *PyDUR*3.3 exhibits sporophyte-specific expression that is nutrient deficiency independent; however, nutrient deficiency-inducible expression was observed for *PyDUR*3.1 and *PyDUR*3.2, although they have expressed generation independently and gametophyte specifically, respectively [26] [27]. The expression of *PyAMT*1 is gametophyte specific and is regulated both temporally and by nitrogen deficiency stress [15]. Notably, nitrogen deficiency-inducible expression of *PyAMT*1 is strongly suppressed by addition of NH_4^+ compared to urea and other amino acid compounds [15].

These findings led us to hypothesize the presence of an AMT gene family in *P. yezoensis*, possibly with differential regulation of each gene. Here, we demon-

strated that there are indeed multiple AMT1 genes in *P. yezoensis*, with diversity in both phylogenetic relationships with other plant and algal AMTs and expression patterns during the life cycle and under nitrogen-deficient conditions

2. Materials and Methods

2.1. Algal Samples and Culture Conditions

Gametophytes, conchosporangia and sporophytes of *Pyropia yezoensis* (strain U-51) were maintained in sterilized artificial seawater (SEALIFE; Marinetech, Tokyo, Japan) enriched with ESS_2 containing $NaNO_3$ as a nitrogen source, vitamins, and trace metal elements (**Table S1**) [28]. The algae were grown under 60 μmol photons·m^{-2}·s^{-1} light in a short-day photoperiod (10 h light/14 h dark) at 15˚C with air filtered through a 0.22-μm filter (Whatman; Maidstone, UK). The culture medium was changed weekly. For nitrogen starvation experiments, gametophytes, conchosporangia and sporophytes were treated with artificial seawater without ESS_2 (free of a nitrogen source) for a week. Algal materials were sampled daily after starting the starvation treatment to measure gene expression.

2.2. Quantification of Photosynthetic Pigments

Gametophytes and sporophytes were treated with N-free (ESS_2-free) seawater for 3, 5 or 7 days to observe discoloration. For recovery from discoloration, gametophytes and sporophytes discolored for a week were transferred into seawater supplied with 500 μM of NH_4Cl, $NaNO_3$, or urea and then cultured for a further week. Discolored and recovered samples (0.1 g fresh weight per sample) were used to calculate chlorophyll *a* (Chl *a*) contents according to Seely *et al.* [29] and phycoerythrin (PE) and phycocyanin (PC) contents as described by Beer and Eshel [30].

2.3. Identification and Characterization of AMTs

Unigenes annotated as putative AMT*s* were selected from our transcriptome analyses of *P. yezoensis* [31], and their identity was confirmed by comparison of predicted amino acid sequences with those of known AMTs by a BLAST search (https://blast.ncbi.nlm.nih.gov/Blast.cgi) after identification of full-length open reading frames (ORFs) with the ORF finder (https://www.ncbi.nlm.nih.gov/orffinder/). The ProtParam tool (https://web.expasy.org/protparam/) was used to predict the molecular weights, theoretical isoelectric point (pI), and grand average of hydropathicity (GRAVY). The location of the ammonium transporter (AMT) domain was identified with Pfam (http://pfam.xfam.org/search#tabview=tab0), and transmembrane helices in the conserved AMT domain were predicted using a SMART search (http://smart.embl-heidelberg.de). In addition, three-dimensional structures of AMT domain-containing proteins were predicted with the Phyre2 Server (http://www.sbg.bio.ic.ac.uk/phyre2/html/).

2.4. Phylogenetic Analysis

AMTs used for the phylogenetic analysis were obtained from GenBank, genome and EST databases and our unpublished transcriptome analyses are listed in Table S2 with their accession numbers and gene IDs. These included AMTs from Streptophyta (*Arabidopsis thaliana*, https://www.arabidopsis.org; *Physcomitrella patens*, https://genome.jgi.doe.gov/Phypa1_1/Phypa1_1.home.html), Rhodophyta (*Porphyra umbilicalis*, https://phytozome.jgi.doe.gov/pz/portal.html#; *Porphyra purpurea*, https://www.ncbi.nlm.nih.gov/sar/SRX100230; *Porphyridium purpureum*, http://cyanophora.rutgers.edu/porphyridium/; *Cyanidioschyzon merolae*, http://merolae.biol.s.u-tokyo.ac.jp; *Galdieria sulphuraria*, http://plants.ensembl.org/Galdieria_sulphuraria/Info/Index), Chlorophyta (*Chlamydomonas reinhardtii*, https://genome.jgi.doe.gov/Chlre4/Chlre4.home.html; *Volvox carteri f. nagariensis*, https://www.uniprot.org/proteomes/UP000001058), and Heterokontophyta (*Phaeodactylum tricomutum*, https://genome.jgi.doe.gov/Phatr2/Phatr2.home.html; *Cylindrotheca fusiformis*, https://www.uniprot.org/uniprot/?query=cylindrotheca+fusiformis&sort=score). A neighbor-joining phylogenetic tree was constructed with MEGA 7 software (https://www.megasoftware.net) using ClustalW to align the AMT amino acid sequences.

2.5. Total RNA Extraction and cDNA Synthesis

Total RNA was separately extracted from gametophytes, conchosporangia and sporophytes using the RNeasy Plant Mini Kit (Qiagen, Hilden, Germany) and then treated with DNase (TURBO DNA-free TM kit, Invitrogen, Carlsbad, USA) to remove genomic DNA contamination. Then, first-stand complementary DNA (cDNA) was synthesized from 300 ng of total RNA with the PrimeScript 1st strand cDNA Synthesis Kit (TaKaRa Bio, Kusatsu, Japan) according to the manufacturer's instructions. Before being used as a template in quantitative PCR (qPCR) analyses, the quality of the cDNA was evaluated by amplification of the *P. yezoensis* 18*S* rRNA gene with its gene primer set (Table S3) [27] via PCR reactions with Phusion high-fidelity DNA polymerase with GC buffer (Biolabs, Massachusetts, USA) according to the manufacturer's instructions. The thermal cycling parameters consisted of an initial denaturation step 98˚C for 30 s, and 30 cycles of 98˚C for 10 s, 60˚C for 30 s and 72˚C for 20 s, and a final extension step 72˚C for 5 mins.

2.6. Gene Expression Analysis

Primers for qPCR were designed using Primer Premier 5 software (http://www.premierbiosoft.com) and are listed in Table S3. To confirm the sizes of amplified products and applicability of primers, a mixture of three cDNA samples was used with all primer sets for PCR with Phusion high-fidelity DNA polymerase and GC buffer (Biolabs, Massachusetts, USA) according to the manufacturer's instructions. PCR products were checked by agarose gel electropho-

resis. Primer sets that amplified DNA bands with expected sizes were employed for the qPCR. qPCR was carried out in a total volume of 20 µl containing 10 µl of 2 × SYBR Premix Ex Taq GC, 0.4 µl of ROX Reference Dye, 2 µl of cDNA template, and 0.4 µl (10 µM) of each primer, using the SYBR Premix Ex Taq GC kit (Takara Bio, Kusatsu, Japan). The thermal cycling parameters consisted of 95˚C for 5 min and 40 cycles of 94˚C for 30 s, 60˚C for 30 s and 72˚C for 20 s. The dissociation curve was generated by heating from 60 to 95˚C to check for specificity of amplification using an Applied Biosystems 7300 real-time PCR system (Life Technologies, Carlsbad, USA). The data were examined with one-way ANOVA, and the level of significance was defined at $P < 0.05$.

3. Results

3.1. A multiplicity of *P. yezoensis* AMT Genes

Based on the functional annotation in our *P. yezoensis* transcriptome analysis [31], we identified six unigenes (CL1839, CL3739, Unigene15210, CL1882. Contig5, CL1882. Contig6 and Unigene24155) as candidate *P. yezoensis* AMT (*PyAMT*) genes, in addition to the known *PyAMT*1 [15]. These six additional unigenes contained predicted open reading frames (ORFs) encoding 484, 654, 589, 616, 690, and 522 amino acid products (**Figure 1**) with molecular masses of 51.2, 67.8, 58.67, 63.68, 72.06, and 53.78 kDa, respectively, and all contained the conserved AMT domain (**Table S4**). In addition, CL1839, CL3739, Unigene15210, CL1882. Contig5, CL1882. Contig6 and Unigene24155 showed 55.04%, 32.42%, 38.07%, 27.77%, 25.36%, and 16.88% identity to *PyAMT*1, respectively. Based on these findings, we concluded that all of the candidates are likely to be AMTs. However, the product of Unigene 24155 had 12 predicted transmembrane (TM) helixes in contrast to the products of the other candidate genes, which had 11 TM helixes (**Table S5**), suggesting a structural difference in Unigene24155 from the other genes. Other structural characteristics of these gene products, including a total number of atoms and theoretical pI, are listed in **Table S4**.

The crystal structure of the ammonium transporter protein in *Escherichia coli* (AmtB) revealed that two phenylalanine residues, Phe107 and Phe215, block the hydrophobic NH_4^+ conduction pore, and two highly conserved histidine residues, His168 and His318, maintain the shape of the central pore involved in NH_4^+ transport [32] [33]. As shown in **Figure 1**, these four sites were highly conserved in *P. yezoensis* AMTs. In addition, in consistent with Kakinuma *et al.* [15], a tripeptide sequence, Phe-Gly-Phe (Tyr/Asn), indicating AMT identity, was found in all of the *PyAMT*s (**Figure 1**). Moreover, three-dimensional structures predicted *in silico* for all of *P. yezoensis* AMT domain-containing proteins were similar to those of known AMTs. Indeed, crystal structures of 5 *PyAMT*s (*PyAMT*1, CL1839, Unigene 15210, CL1882. Contig5, CL1882. Contig6) structurally resembled that of the AMT template c5aexB (*Saccharomyces cerevisiae* MEP2), while CL3739 was quite similar to the other AMT template c5aezA (*Candida albicans* MEP2) (**Figure 2**). Moreover, three-dimensional structures of Unigene24155 were closely related to that of the template c3hd6A (human rhesus

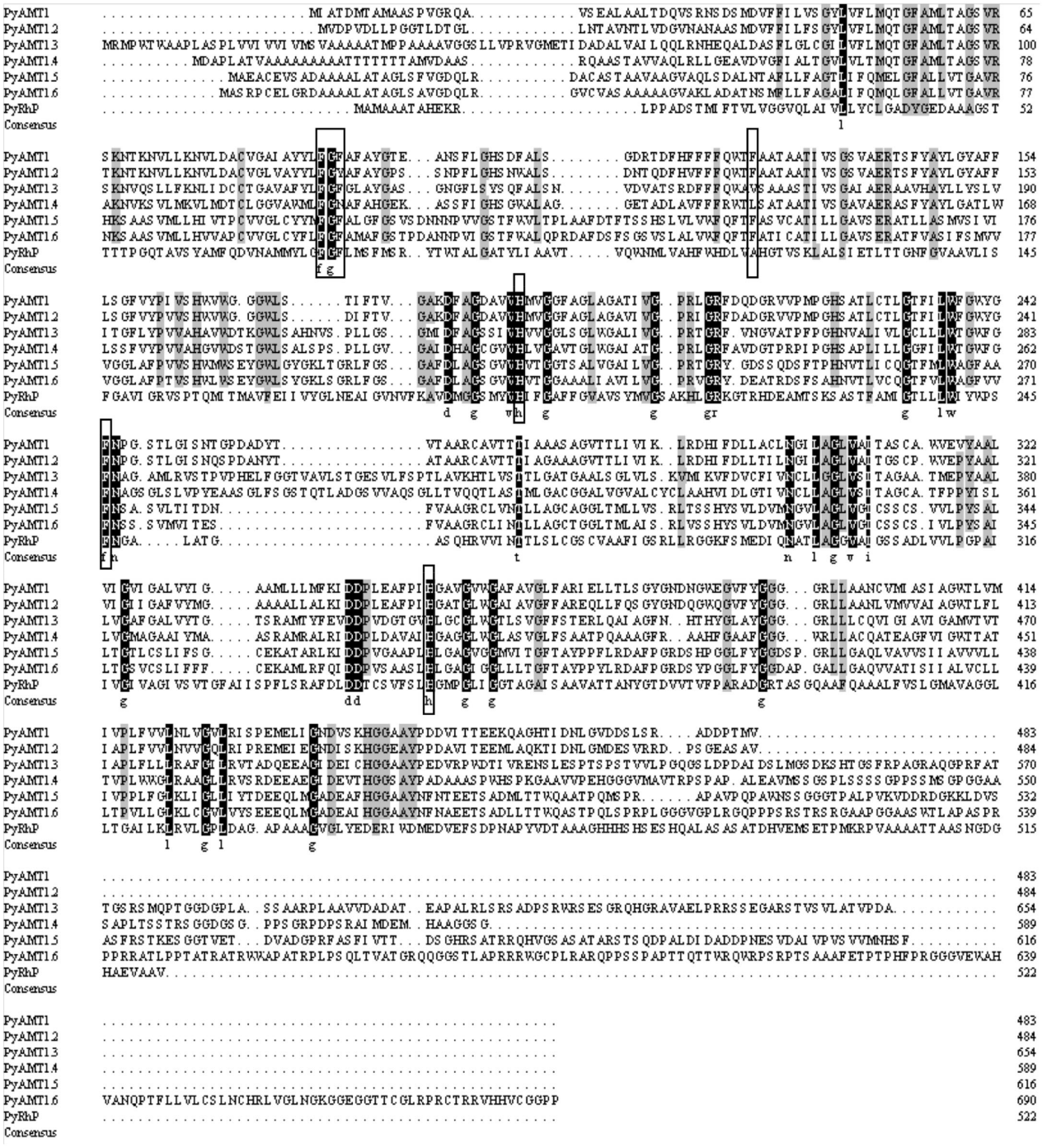

Figure 1. Conservation of AMT identity among six *PyAMT*1s and *PyRh*. Amino acid residues conserved in all seven proteins and in six proteins are highlighted by black (with white characters) and gray backgrounds, respectively. The boxes indicate the Phe-Gly-Phe (Tyr/Asn) triplet conserved in AMTs, as well as phenylalanine and histidine residues corresponding to residues involved in NH_4^+ binding and transport in *E. coli* EcAmtB. The amino acid numbers are indicated on the right.

protein, Rh, structurally related to AMT) (**Figure 2**). Taken together with characteristics in primary sequences (**Figure 1**), these findings highly suggested functional NH_4^+-transport and Rh activities of AMT domain-containing proteins from *P. yezoensis*.

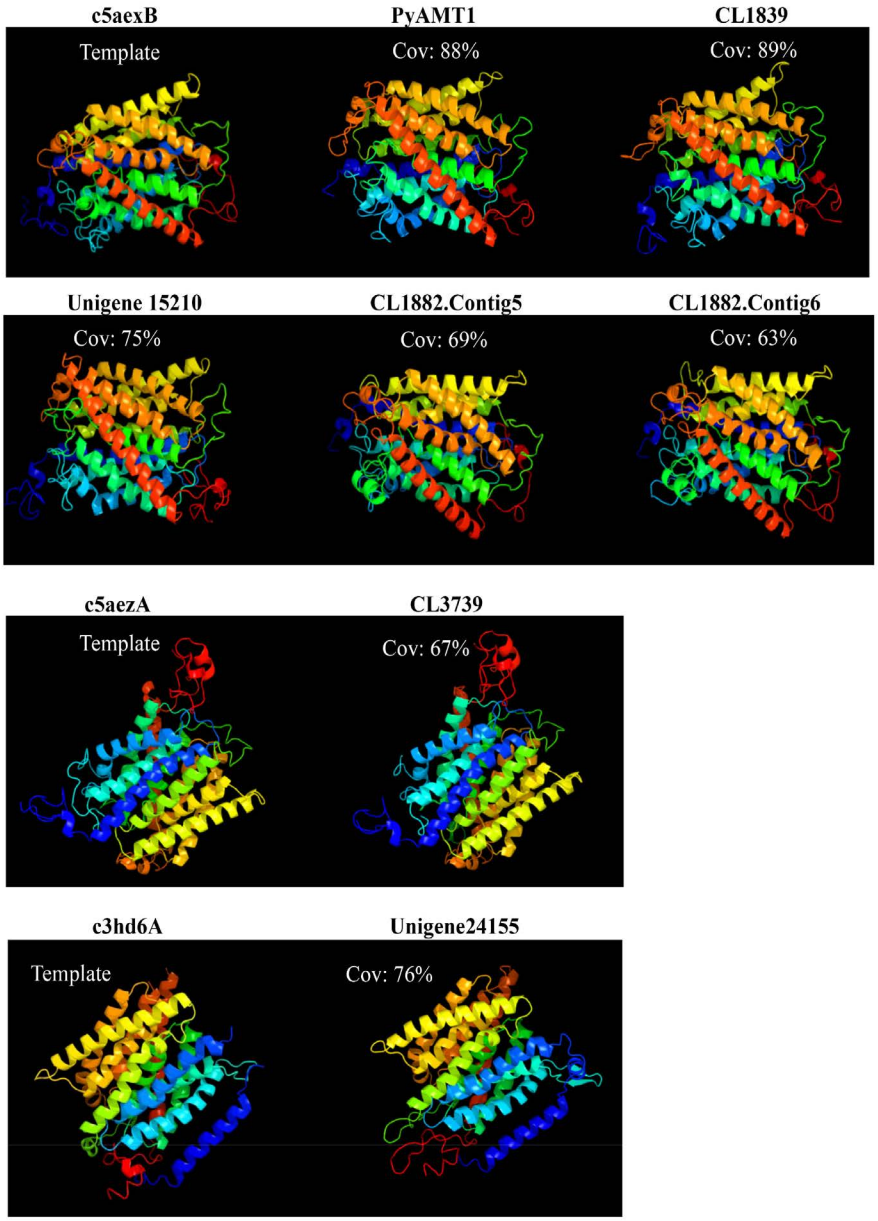

Figure 2. High degree of similarity in three-dimensional structures between AMT domain-containing proteins from *P. yezoensis* and known AMTs. Templates c5aexB and c5aezA indicate three-dimensional structures of AMTs (MEP2s) from *Saccharomyces cerevisiae* and *Candida albicans*, respectively, while c3hd6A represents a three-dimensional structure of the human rhesus protein (Rh). Cov means the coverage percent of AMT domain-containing proteins to the corresponding templates.

3.2. Phylogenetic Classification of *P. yezoensis* AMTs into AMT1 and Rhesus Protein Subfamilies

To explore what type(s) of AMTs these unigenes encode, we performed a phylogenetic analysis with other full-length amino acid sequences of known AMTs from algae, plants, animals and bacteria. All of the *P. yezoensis* sequences except for Unigene24155 were placed in the plant AMT subfamily 1 clade. Therefore,

we considered these unigenes to encode AMT1s and designated them as *PyAMT*1.2 (CL1839), *PyAMT*1.3 (CL3739), *PyAMT*1.4 (Unigene15210), *PyAMT*1.5 (CL1882. Contig5), and *PyAMT*1.6 (CL1882. Contig6). Unigene24155 shared 27.56% and 24.70% identity with CrRh1 and CrRh2 from the green alga *Chlamydomonas reinhardtii*, respectively, but only 16.88% with *PyAMT*1. Our analysis placed this protein in the Rh clade, which is phylogenetically divergent from both AMT1 and AMT2 clades (**Figure 3**). Rh proteins are homologues of AMT proteins that were first identified in human erythroid cells [34] [35]. The predicted 12 transmembrane helixes of the Unigene24155 protein is in accordance with Rh proteins of other organisms [36] [37]. Thus, we designated Unigene24155 as *PyRh*.

Our phylogenetic analysis also indicated that algal AMTs were mostly classified into the AMT1 subfamily, which is distantly related to the AMT2 subfamily clade. In addition, AMT1s from red algae, green algae, diatoms, and land plants formed independent clades. Thus, an ancient algal AMT1 may have existed prior to the divergence of red and green algae, although the origin of AMT2s is unclear.

The six PyAMT1s were subdivided into three different Rhodophyta clades, each of which contained pairs of *PyAMT*1s: *PyAMT*1 and *PyAMT*1.2, *PyAMT*1.3 and *PyAMT*1.4, and *PyAMT*1.5 and *PyAMT*1.6 (**Figure 3**). In addition, the three Rhodophyta clades also contained pairs of AMT1s from the red seaweed *Porphyra umbilicalis*: The *PyAMT*1/1.2 clade with Pum0126s0003.1 (OSX77964.1), Pum1775s0001.1 (OSX69172.1), Pum0463s0020.1 (OSX72158.1), and Pum0165s0019.1 (OSX77025.2); the PyAMT1.3/1.4 clade with Pum0027s0002.1 (OSX80976.1) and Pum1656s0001.1 (OSX69292.1); and the *PyAMT*1.5/1.6 clade with Pum0022s0083.1 (OSX81363.1) (**Figure 3**). Moreover, AMT1s from Chlorophyta were separated into three different clades, independent from each other and from the three clades of Rhodophyta. Thus, expansion and divergence of the ancient algal AMT1 gene into three groups occurred independently in red and green algae after their establishment.

3.3. Differences in Temporal Expression Patterns of *PyAMT*1 and *PyRh* Genes during the Life Cycle

Figure 4 shows the relative transcript abundance of *PyAMT*1 and *PyRh* genes in the gametophyte, conchosporangium and sporophyte tissues under normal growth conditions. When life cycle specificity of gene expression was compared between the gene pairs found in the three phylogenetic clades, *PyAMT*1 was specifically expressed in the gametophyte, while the expression of *PyAMT*1.2 was found in both the sporophyte and conchosporangium. By contrast, *PyAMT*1.3 and *PyAMT*1.4 exhibited the same sporophyte-dominant expression pattern. *PyAMT*1.6 was expressed constitutively, whereas transcripts of *PyAMT*1.5 were not detectable at any stage (data not shown). Thus, two of the gene pairs in the same clade did not share the same expression pattern. We did not find evidence of *PyRh* expression at any point in the life cycle (data not shown).

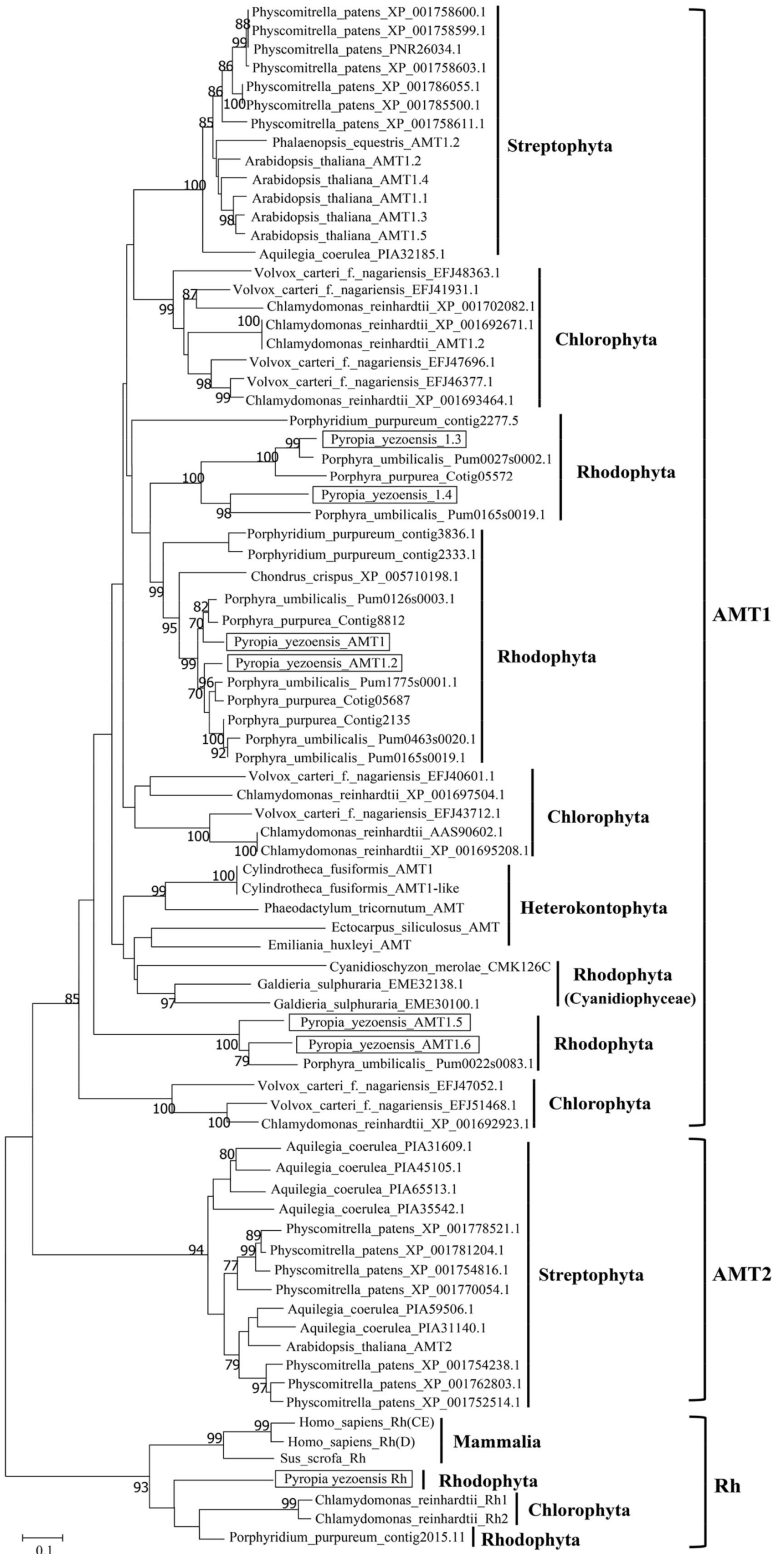

Figure 3. Neighbor joining-based phylogenetic tree of AMTs from terrestrial plants and algae. Boxes indicate *PyAMT*s and *PyRh*. The bootstrap values with 1000 replicate over 70% are indicated at the nodes of the tree. The DDBJ/EMBL/GenBank accession numbers of AMTs and Rhs used in the phylogenetic analysis are listed in **Table S2**.

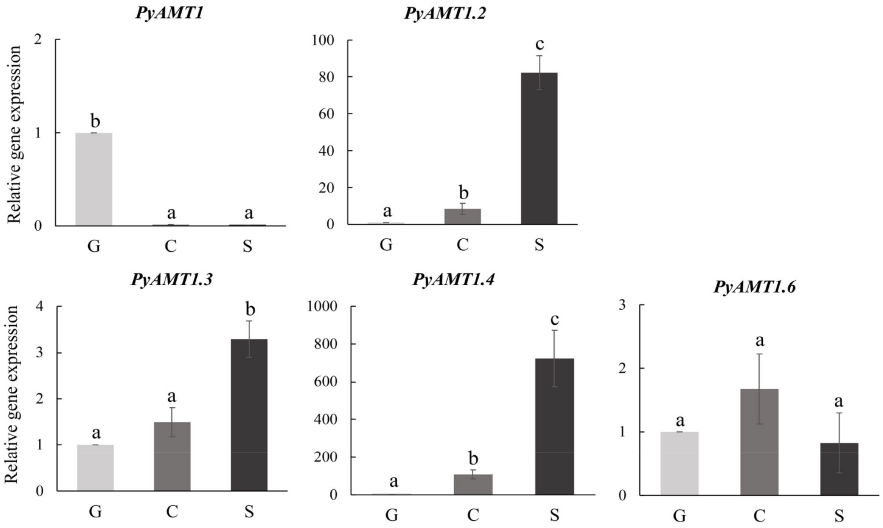

Figure 4. Differences in temporal expression patterns of *PyAMTs* in the life cycle of *P. yezoensis*. The relative mRNA levels of *PyAMT*1*s* were normalized with the reference gene 18*S* rRNA. Error bars indicate the standard deviation of triplicate experiments (n = 3), and different letters on bars indicate significant differences at $P < 0.05$ tested with ANOVA. G, gametophyte; C, conchosporangium; S, sporophyte.

3.4. Induction of and Recovery from Discoloration

Gametophyte and sporophyte tissues maintained in the ESS_2-containing seawater were transferred to seawater without ESS_2 and cultivated for an additional 3, 5 or 7 days. As results, discoloration was initially observed after 3 days and gradually strengthened until 7 days in both gametophytes and sporophytes (**Figure 5**). Correspondingly, the contents of photosynthetic pigments Chl *a*, PE and PC were decreased respectively in gametophytes from 1.37 to 0.40, 6.42 to 3.18, and 1.27 to 0.35 $mg \cdot g^{-1}$ FW and in sporophyte from 1.49 to 0.58, 5.24 to 1.99, and 0.48 to 0.18 $mg \cdot g^{-1}$ FW (**Figure 6**). To examine recovery from discoloration, 7-day-discolored gametophytes and sporophytes were treated with nutrition-deficient medium containing 500 μM NH_4Cl, $NaNO_3$, or urea for a week. As shown in **Figure 5**, discoloration was recovered visibly, which was supported by the increase in the contents of Chl *a*, PE and PC to the levels corresponding to those in non-discolored gametophytes and sporophytes (**Figure 6**). These findings suggested essential roles of the AMT activity for recovery from discoloration in *P. yezoensis*.

3.5. Diversity in the Nutrition Starvation-Inducible Pattern of *PyAMT*1 Subfamily Genes during the Life Cycle

We examined the nitrogen deficiency-inducible expression of the *PyAMT*1 genes. As shown in **Figure 7**, all *PyAMT*1 genes displayed nitrogen deficiency-inducible expression without alterations in their life cycle stage specificity. However, the expression patterns differed among the genes. For instance, transient induction in gametophytes was observed for *PyAMT*1, *PyAMT*1.2, and *PyAMT*1.3, whereas expression of *PyAMT*1.2 and *PyAMT*1.4 gradually increased in both

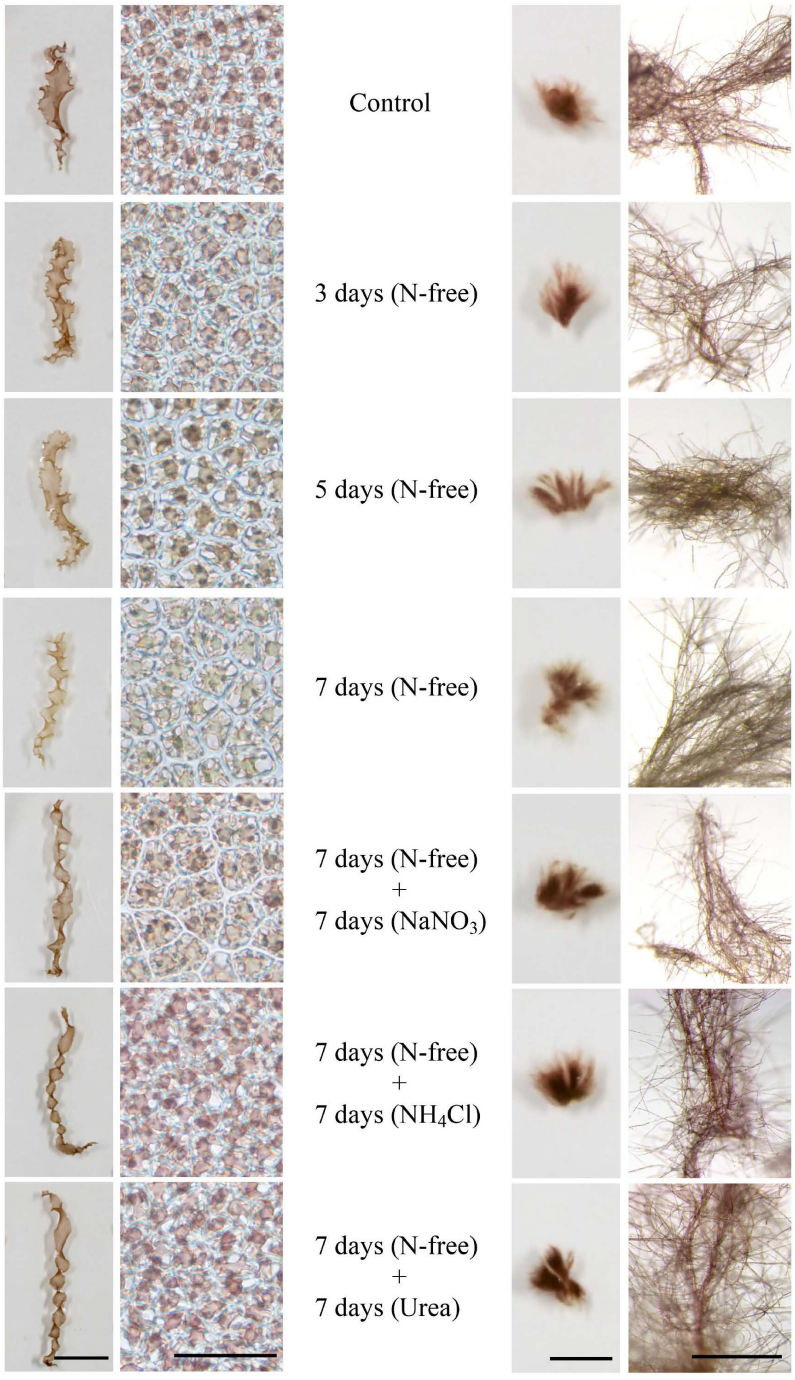

Figure 5. Artificial induction of and recovery from discoloration in *Pyropia yezoensis*. Gametophytes (left) and sporophytes (right) were treated with N-free (ESS_2-free) seawater for a week, and sampling was performed at 3, 5 and 7 days to observe discoloration. Control indicates samples cultured in ESS_2-enriched seawater. In addition, discolored gametophyte and sporophytes produced in N-free seawater for 7 days were transferred into ESS_2-less seawater supplied with 500 μM of NH_4Cl, $NaNO_3$, or urea and then cultured for an additional 7 days to examine the recovery from discoloration. Scale bars in left and right panels indicate 1 cm and 50 μm in gametophytes and 1 cm and 500 μm in sporophytes.

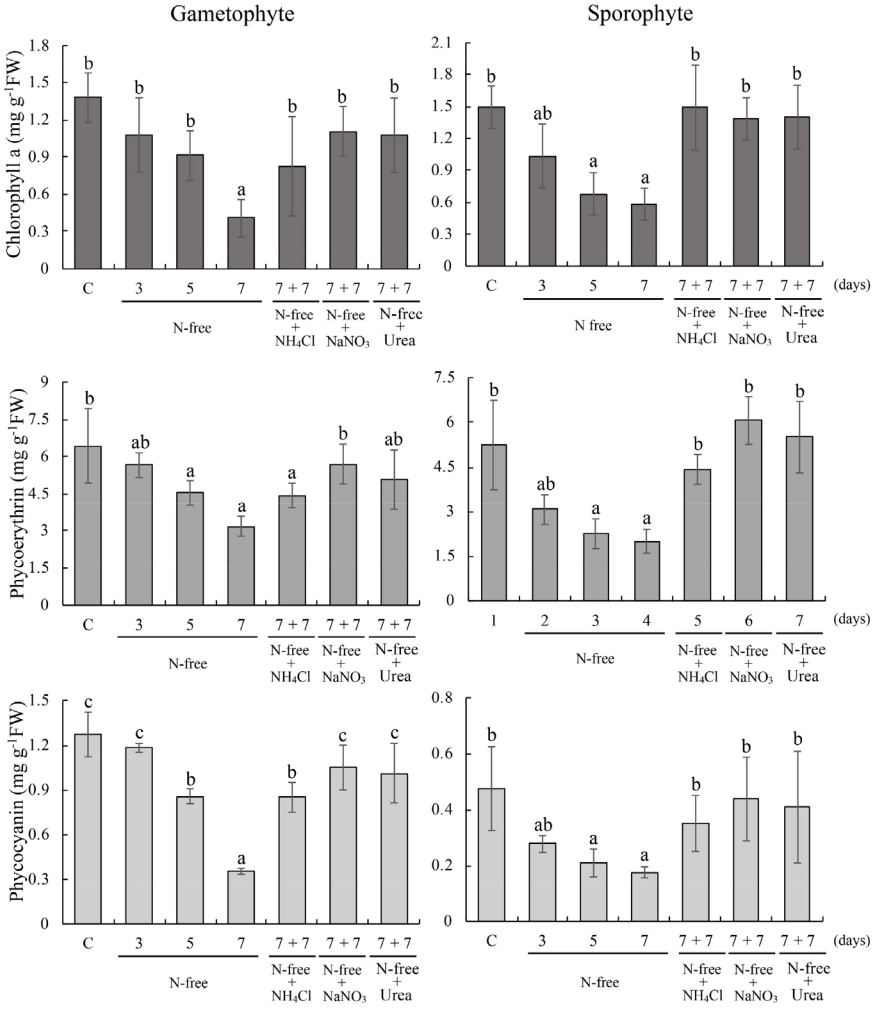

Figure 6. Changes in the contents of chlorophyll a, phycoerythrin and phycocyanin in discolored and recovered *P. yezoensis*. Culture conditions were identical to those in **Figure 5**. C means control samples. Error bars indicate the standard deviation of triplicate experiments (n = 3), and different letters on bars indicate significant differences at $P < 0.05$ tested with ANOVA.

conchosporangia and sporophytes. Moreover, the *PyAMT*6 expression gradually increased in gametophyte tissue, and transient expression of *PyAMT*6 was observed in conchosporangia and sporophytes. Transcripts of *PyAMT*1.5 and *PyRh* remained undetectable in all tissues evaluated, even under nitrogen-deficient conditions (data not shown).

We further examined the expression of the *PyAMT*1 genes to determine the effects of nitrogen recovery on their expression. For these experiments, we selected *PyAMT*1.2 and *PyAMT*1.4, whose expression continually increased in sporophytes under nitrogen deficiency. When discolored sporophytes produced by 7-day culture in the ESS_2-less medium were transferred to ESS_2-less medium containing 500 μM NH_4Cl and further cultured for 3 days, the expression of the two genes was strongly down-regulated within 24 h ($P < 0.05$; **Figure 8**). In addition, the same effect was observed in ESS_2-less medium containing 500 μM

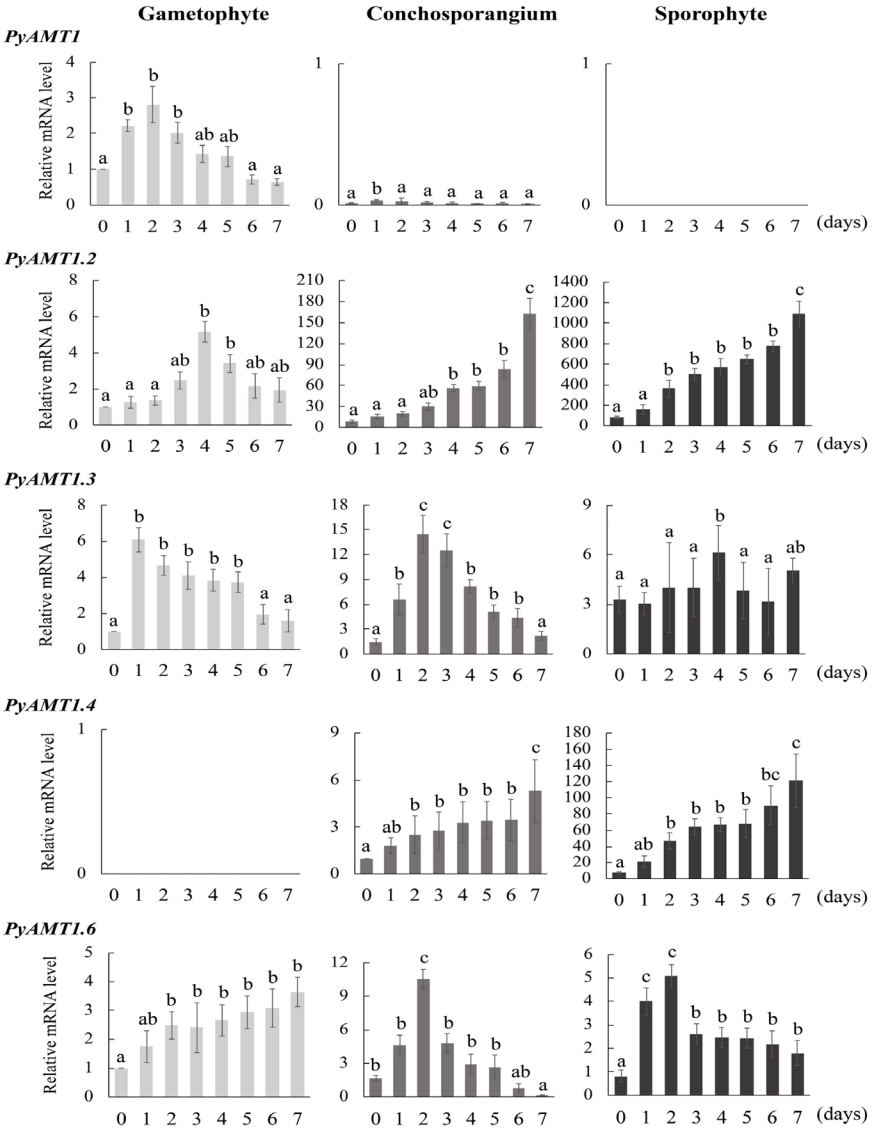

Figure 7. Differences in nitrogen starvation-induced expression patterns among *PyAMT1* genes. Samples of gametophytes, conchosporangia, and sporophytes treated with ESS_2-free seawater were collected every day for 7 days to examine the expression of the *PyAMT1* genes by qRT-PCR. The relative mRNA levels were normalized with the reference gene 18S rRNA. Error bars indicate the standard deviation of triplicate experiments (n = 3), and different letters on bars indicate significant differences at $P < 0.05$ tested with ANOVA. G, gametophyte; C, conchosporangium; S, sporophyte. The numbers on the X-axis indicate the duration of culture under nitrogen-deficient conditions (days).

$NaNO_3$ or 500 μM urea (Figure 8). These results were consistent with the previous observation [15] that *PyAMT*1 gene expression is down-regulated by the addition of inorganic and organic nitrogen sources.

4. Discussion

A NH_4^+ is an important nitrogen source that is transported via AMTs, which are ubiquitous plasma membrane proteins and are classified into three subfamilies,

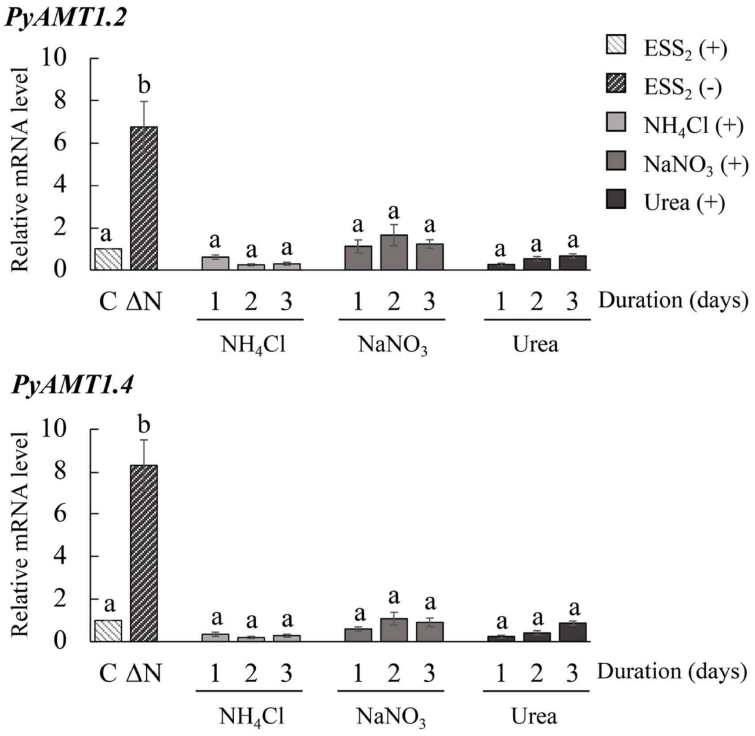

Figure 8. Suppression of the nitrogen starvation-induced expression of *PyAMT*1 genes via recovery with different nitrogen sources. Sporophyte samples grown in ESS_2-less seawater for 7 days (ΔN) were treated with seawater containing 500 μM of NH_4Cl, $NaNO_3$, or urea for 3 days. Sporophytes cultured in nitrogen-supplied seawater were collected every day for 3 days, and the expression of *PyAMT*1.2 and *PyAMT*1.4 was examined by qRT-PCR (upper and lower, respectively). The relative mRNA levels were normalized with the reference gene *18S* rRNA. Error bars indicate the standard deviation of triplicate experiments (n = 3), and different letters on bars indicate significant differences at $P < 0.05$ tested with ANOVA. S, sporophytes cultured in ESS_2-containing seawater. The numbers on the X-axis indicate the duration of culture under nitrogen-deficient conditions (days).

AMT1, AMT2 and Rh [38]. Although the structure, expression patterns and physiological roles of AMT genes have been well studied in animals and land plants [2] [13] [34] [39], algal AMT genes remain poorly understood. Here, we report the presence of the AMT1 and Rh gene subfamilies in *P. yezoensis* and the diversity in their expression patterns.

Our phylogenetic analysis demonstrated the diversity of the AMT1 subfamily, consisting of independent phylum-specific clades (**Figure 3**). Land plants have their own AMT1 subfamily, with five genes in *Arabidopsis* [4] [11] [12] [13], at least 10 genes in rice [9], and 23 genes in wheat [8]. Although AMT1s from land plants formed a single clade, it was separated from the algal AMT1 subfamily, in which the unicellular green algae *C. reinhardtii* and the red seaweed *Po. umbilicalis* have 11 and 7 AMT1 genes, respectively [18] [21], in addition to the 6 *PyAMT*1 genes. AMTs in *Po. umbilicalis* have been annotated as AMT1, AMT2, and AMT3 by Brawley *et al.* [21]. Despite these names, our phylogenetic

analysis indicated that all of the AMTs in *Po. umbilicalis* are AMT1 subfamily members (PuAMT1s) as are other algal genes (**Figure 3**). Moreover, the six *PyAMT*1s and seven PuAMT1s were subdivided into three groups (**Figure 3**). The existence of multiple independent AMT1 clades in *P. yezoensis* and *Po. umbilicalis* is the distinguishing characteristic of AMT1s from Bangiales, since AMT1s from land plants formed a single clade (**Figure 3**). These findings imply that an ancient red algal AMT gene may have diversified into three genes prior to the separation of *Pyropia* and *Porphyra*, and then further diversification occurred independently for each of the three genes in these species.

Similar to Rhodophyta, AMT1s of Chlorophyta were divided into three groups, although their phylogenetic positions were different from the Rhodophyta clades (**Figure 3**). This result is in agreement with the report that three subfamilies of CrAMT1s have been established in *Chlamydomonas* [3]. Therefore, a two-step diversification of algal AMT1s has been proposed: An early expansion of the ancient algal gene into three variants prior to the divergence of Chlorophyta and Rhodophyta and a late duplication of each of the three variants after the divergence of the green and red lineages.

The multiplicity of AMT1 genes in Chlorophyta and Rhodophyta points to functional divergence of these genes in seaweeds. This hypothesis is supported by our gene expression analyses indicating differences in temporal and nitrogen stress-inducible expression patterns for the *PyAMT*1 genes (**Figure 7** and **Figure 8**). *PyAMT*1, *PyAMT*1.3, and *PyAMT*1.4 commonly exhibited a transient increase in their expression under nitrogen-deficient conditions, although differences were observed in their life cycle stage-specific expression. Thus, it seems that functional divergence in *PyAMT*1s might allow for functional specialization over a range of NH_4^+ concentrations, which would enable *P. yezoensis* to react appropriately to a wide range of NH_4^+ concentrations in the environment. In the future, functional analysis of each *PyAMT*1 focused on NH_4^+ uptake under nitrogen deficiency conditions should help us to understand their transport capacity and how *P. yezoensis* responds and adapts to nitrogen deficiency stress during its life cycle.

Nitrogen deficiency results in leaf senescence in land plants [40] [41]. In leaf senescence, nitrogen is reused to support plant growth and reproduction by reallocating from aging leaves to younger tissues [8] [9] and degradation of chlorophylls and following discoloration of tissues occur in aging leaves [42] [43]. Thus, loss of nitrogen and degradation of photosynthetic pigments are responsible for leaf senescence [40] [44]. In macroalgae, nitrogen plays an important role in producing amino acids and photosynthetic pigments such as Chl *a*, PE and PC [45]. As shown in **Figure 5** and **Figure 6**, nitrogen deficiency-induced discoloration by reducing these three photosynthetic pigments in *P. yezoensis*. Given the simple architecture of the thallus and conchocelis and the fact that discoloration was observed throughout the entire organism (**Figure 5**), reallocation of nitrogen is not responsible for the discoloration in *P. yezoensis*, suggesting that the mechanism behind the discoloration caused by nitrogen starvation is

different from that in land plants, although loss of photosynthetic pigments in discoloration is common.

The discoloration in *P. yezoensis* thalli was rescued and the mRNA level of *PyAMT*1 was down-regulated by an increase in the concentrations of not only inorganic but also organic nitrogen sources [15]. Similarly, nitrogen deficiency-inducible discoloration and the expression of *PyAMT*1.2 and *PyAMT*1.4 in the sporophyte were also strongly repressed after addition of NH_4Cl, $NaNO_3$, and urea in the culture medium (**Figure 8**). Since inorganic and organic nitrogen sources are metabolized into NH_4^+ to assimilate the nitrogen into cellular components [46] [47], $NaNO_3$ and urea might increase the intracellular NH_4^+ contents and similarly affect the expression of *PyAMT*1 genes. These findings indicated that discoloration in *P. yezoensis* during nitrogen starvation is induced by the decreased extracellular nitrogen content, although leaf senescence in land plants occurs as a result of nitrogen reallocation between different tissues [48] [49].

Another distinguishing characteristic of algal NH_4^+ transporters is the presence of Rh proteins, such as *PyRh* in *P. yezoensis* and contig2015.11 in *Porphyridium purpureum* (**Figure 3**), which contain the conserved AMT domain but are distantly related to the AMT1 and AMT2 subfamilies [36] [50]. *Rh* split from *AMT* in archaeal species and coexists in microbes and invertebrates, but not in fungi, vascular plants, and vertebrates [50]. To date, *Rh* has not been reported in algae except for CrRh1 and CrRh2 from the green alga *C. reinhardtii* [37] [51]; our findings reveal the presence of *Rh* in red algae (**Figure 3**). Although the expression of *CrRh*1 and *CrRh*2 is regulated by CO_2 [37] [51], the expression of *PyRh* was not detected during the life cycle in *P. yezoensis* nor under the nitrogen-deficient conditions (data not shown). Thus, little is known about the physiological functions of Rh proteins in algae.

In conclusion, algal NH_4^+ transporters are divided into the AMT1 and Rh subfamilies. The AMT1 subfamily of *P. yezoensis* consists of three groups containing genes whose expression patterns differ temporally and are nitrogen deficiency-dependent during the life cycle. These findings are novel for algal NH_4^+ transporters, and future work should elucidate the functions of each member of the AMT1 and Rh subfamilies, which could help clarify the unique algal strategies of response and acclimation to nitrogen deficiency stress by phylogenetically independent and diverse AMT1s and Rhs during the life cycle.

Acknowledgements

We are grateful to Mr. Masahiro Suda and Mr. Ryunosuke Irie for their supporting for laboratory culture of *P. yezoensis* gametophytes and sporophytes. Chengze Li was supported by the Ministry of Education, Culture, Sports, Science and Technology of Japan and by the China Scholarship Council.

Conflicts of Interest

The authors declare no conflicts of interest regarding the publication of this paper.

References

[1] Nicolaus, W., Sonia, G., Alain, G. and Frommer, W.B. (2000) The Molecular Physiology of Ammonium Uptake and Retrieval. *Current Opinion in Plant Biology*, **3**, 254-261.

[2] Couturier, J., Montanini, B., Martin, F., Brun, A., Blaudez, D. and Chalot, M. (2007) The Expanded Family of Ammonium Transporters in the Perennial Poplar Plant. *New Phytologist*, **174**, 137-150. https://doi.org/10.1111/j.1469-8137.2007.01992.x

[3] González-Ballester, D., Camargo, A. and Fernández, E. (2005) Ammonium Transporter Genes in *Chlamydomonas*: The Nitrate-Specific Regulatory Gene *Nit2* Is Involved in *Amt*1*;* 1 Expression. *Plant Molecular Biology*, **56**, 863-878. https://doi.org/10.1007/s11103-004-5292-7

[4] Gazzarrini, S., Lejay, L., Gojon, A., Ninnemann, O., Frommer, W.B. and Wiréna, N. (1999) Three Functional Transporters for Constitutive, Diurnally Regulated, and Starvation-Induced Uptake of Ammonium into Arabidopsis Roots. *The Plant Cell*, **11**, 937-947. https://doi.org/10.1105/tpc.11.5.937

[5] Ludewig, U., Neuhauser, B. and Dynowski, M. (2007) Molecular Mechanisms of Ammonium Transport and Accumulation in Plants. *FEBS Letters*, **581**, 2301-2308. https://doi.org/10.1016/j.febslet.2007.03.034

[6] D'Apuzzo, E., Rogato, A., Simon-Rosin, U., Alaoui, H.E., Barbulova, A., Betti, M., *et al.* (2004) Characterization of Three Functional High-Affinity Ammonium Transporters in Lotus Japonicus with Differential Transcriptional Regulation and Spatial Expression. *Plant Physiology*, **134**, 1763-1774. https://doi.org/10.1104/pp.103.034322

[7] Wittgenstein, N., Le, C.H., Hawkins, B.J. and Ehlting, J. (2014) Evolutionary Classification of Ammonium, Nitrate, and Peptide Transporters in Land Plants. *BMC Evolutionary Biology*, **14**, 1-17. https://doi.org/10.1186/1471-2148-14-11

[8] Li, T., Liao, K., Xu, X., Gao, Y., Wang, Z., Zhu, X., *et al.* (2017) Wheat Ammonium Transporter (AMT) Gene Family: Diversity and Possible Role in Host-Pathogen Interaction with Stem Rust. *Frontiers in Plant Science*, **8**, 1637. https://doi.org/10.3389/fpls.2017.01637

[9] Li, C., Tang, Z., Wei, J., Qu, H., Xie, Y. and Xu, G. (2016) The *OsAMT*1.1 Gene Functions in Ammonium Uptake and Ammonium-Potassium Homeostasis over Low and High Ammonium Concentration Ranges. *Journal of Genetics and Genomics*, **43**, 639-649. https://doi.org/10.1016/j.jgg.2016.11.001

[10] Zhang, F., Liu, Y., Wang, L., Bai, P., Ruan, L., Zhang, C., *et al.* (2018) Molecular Cloning and Expression Analysis of Ammonium Transporters in Tea Plants (*Camellia sinensis* (L.) O. Kuntze) under Different Nitrogen Treatments. *Gene*, **658**, 136-145. https://doi.org/10.1016/j.gene.2018.03.024

[11] Yuan, L., Loque, D., Kojima, S., Rauch, S., Ishiyama, K., Inoue, E., *et al.* (2007) The Organization of High-Affinity Ammonium Uptake in *Arabidopsis* Roots Depends on the Spatial Arrangement and Biochemical Properties of AMT1-Type Transporters. *The Plant Cell Online*, **19**, 2636-2652. https://doi.org/10.1105/tpc.107.052134

[12] Yuan, L., Graff, L., Loqué, D., Kojima, S., Tsuchiya, Y.N., Takahashi, H., *et al.* (2009) AtAMT1; 4, a Pollen-Specific High-Affinity Ammonium Transporter of the Plasma Membrane in Arabidopsis. *Plant and Cell Physiology*, **50**, 13-25. https://doi.org/10.1093/pcp/pcn186

[13] Loque, D., Yuan, L., Kojima, S., Gojon, A., Wirth, J., Gazzarrini, S., *et al.* (2006) Additive Contribution of AMT1; 1 and AMT1; 3 to High-Affinity Ammonium Uptake Across the Plasma Membrane of Nitrogen-Deficient Arabidopsis Roots. *The Plant*

Journal, **48**, 522-534. https://doi.org/10.1111/j.1365-313X.2006.02887.x

[14] Giehl, R.F.H., Laginha, A.M., Duan, F., Rentsch, D., Yuan, L. and Wiren, N. (2017) A Critical Role of AMT2; 1 in Root-to-Shoot Translocation of Ammonium in Arabidopsis. *Molecular Plant*, **10**, 1449-1460. https://doi.org/10.1016/j.molp.2017.10.001

[15] Kakinuma, M., Nakamoto, C., Kishi, K., Coury, D.A., Amano, H. (2017) Isolation and Functional Characterization of an Ammonium Transporter Gene, *PyAMT*1, Related to Nitrogen Assimilation in the Marine Macroalga *Pyropia yezoensis* (Rhodophyta). *Marine Environmental Research*, **128**, 76-87. https://doi.org/10.1016/j.marenvres.2016.08.007

[16] Amano, H., Noda, H. (1987) Effect of Nitrogenous Fertilizers on the Recovery of Discoloured Fronds of *Porphyra yezoensis*. *Botanica Marina*, **30**, 467-473. https://doi.org/10.1515/botm.1987.30.6.467

[17] Sakaguchi, K., Ochiai, N., Park, C.S., Kakinuma, M. and Amano, H. (2002) Evaluation of Discoloration in Harvested Laver *Porphyra yezoensis* and Recovery after Treatment with Ammonium Sulfate Enriched Seawater. *Nippon Suisan Gakkaishi*, **69**, 399-404. https://doi.org/10.2331/suisan.69.399

[18] Merchant, S.S., Prochnik, S.E., Vallon, O., Harris, E.H., Karpowicz, S.J., Witman, G.B., *et al.* (2007) The Chlamydomonas Genome Reveals the Evolution of Key Animal and Plant Functions. *Science*, **318**, 245-251. https://doi.org/10.1126/science.1143609

[19] Prochnik, S.E., Umen, J., Nedelcu, A.M., Hallmann, A., Miller, S.M., Nishii, I., *et al.* (2010) Genomic Analysis of Organismal Complexity in the Multicellular Green Alga *Volvox carteri*. *Science*, **329**, 223-226. https://doi.org/10.1126/science.1188800

[20] Schonknecht, G., Chen, W.H., Ternes, C.M., Barbier, G.G., Shrestha, R.P., Stanke, M., *et al.* (2013) Gene Transfer from Bacteria and Archaea Facilitated Evolution of an Extremophilic Eukaryote. *Science*, **339**, 1207-1210. https://doi.org/10.1126/science.1231707

[21] Brawley, S.H, Blouin, N.A., Ficko-Blean, E., Wheeler, G.L., Lohr, M., Goodson, H.V., *et al.* (2017) Insights into the Red Algae and Eukaryotic Evolution from the Genome of *Porphyra umbilicalis* (Bangiophyceae, Rhodophyta). *Proceedings of the National Academy of Sciences*, **114**, 6361-6370. https://doi.org/10.1073/pnas.1703088114

[22] Hildebrand, M. (2005) Cloning and Functional Characterization of Ammonium Transporters from the Marine Diatom *Cylindrotheca fusiformis* (Bacillariophyceae). *Journal of Phycology*, **41**, 105-113. https://doi.org/10.1111/j.1529-8817.2005.04108.x

[23] Eriksen, R.L. and Klein, A.S. (2018) Organism-Environment Interactions and Differential Gene Expression Patterns among Open-Coastal and Estuarine Populations of *Porphyra umbilicalis* Kützing (Rhodophyta) in the Northwest Atlantic. *Fisheries and Aquatic Sciences*, **21**, 28. https://doi.org/10.1186/s41240-018-0103-2

[24] Takahashi, M. and Mikami, K. (2017) Oxidative Stress Promotes Asexual Reproduction and Apogamy in the Red Seaweed *Pyropia yezoensis*. *Frontiers in Plant Science*, **8**, 62. https://doi.org/10.3389/fpls.2017.00062

[25] Adams, E., Mikami, K. and Shin, R. (2017) Selection and Functional Analysis of a *Pyropia yezoensis* Ammonium Transporter PyAMT1 in Potassium Deficiency. *Journal of Applied Phycology*, **29**, 2617-2626. https://doi.org/10.1007/s10811-017-1196-1

[26] Kakinuma, M., Coury, D.A., Nakamoto, C., Sakaguchi, K. and Amano, H. (2008)

Molecular Analysis of Physiological Responses to Changes in Nitrogen in a Marine Macroalga, *Porphyra yezoensis* (Rhodophyta). *Cell Biology and Toxicology*, **24**, 629-639. https://doi.org/10.1007/s10565-007-9053-7

[27] Kakinuma, M., Suzuki, K., Iwata, S., Coury, D.A., Iwade, S. and Mikami, K. (2015) Isolation and Characterization of a New DUR3-Like Gene, *PyDUR*3.3, from the Marine Macroalga *Pyropia yezoensis* (Rhodophyta). *Fisheries Science*, **82**, 171-184. https://doi.org/10.1007/s12562-015-0947-7

[28] Takahashi, M., Saga, N. and Mikami, K. (2010) Photosynthesis-Dependent Extracellular Ca^{2+} Influx Triggers an Asexual Reproductive Cycle in the Marine Red Macroalga *Porphyra yezoensis*. *American Journal of Plant Science*, **1**, 1-11. https://doi.org/10.4236/ajps.2010.11001

[29] Seely, G.R., Duncan, M.J. and Vidaver, W.E. (1972) Preparative and Analytical Extraction of Pigments from Brown Algae with Dimethyl Sulfoxide. *Marine Biology*, **12**, 184-188. https://doi.org/10.1007/BF00350754

[30] Beer, S. and Eshel, A. (1985) Determining Phycoerythrin and Phycocyanin Concentrations in Aqueous Crude Extracts on Red Algae. *Marine and Freshwater Research*, **36**, 785-792. https://doi.org/10.1071/MF9850785

[31] Mikami, K., Li, C., Irie, R. and Hama, Y. (2019) A Unique Life Cycle Transition in the Red Seaweed *Pyropia yezoensis* Depends on Apospory. *Communication Biology*, **2**, 299. https://doi.org/10.1038/s42003-019-0549-5

[32] Soupene, E., Chu, T., Corbin, R.W., Hunt, D.F. and Kustu, S. (2002) Gas Channels for NH_3: Proteins from Hyperthermophiles Complement an *Escherichia coli* Mutant. *Journal of Bacteriology*, **184**, 3396-3400. https://doi.org/10.1128/JB.184.12.3396-3400.2002

[33] Zheng, L., Kostrewa, D., Berneche, S., Winkler, F.K. and Li, X.D. (2004) The Mechanism of Ammonia Transport Based on the Crystal Structure of AmtB of *Escherichia coli*. *Proceedings of the National Academy of Sciences*, **101**, 17090-17095. https://doi.org/10.1073/pnas.0406475101

[34] Marini, A.M., Urrestarazu, A., Beauwens, R. and André, B. (1997) The Rh (Rhesus) Blood Group Polypeptides Are Related to NH_4^+ Transporters. *Trends in Biochemical Sciences*, **22**, 460-461. https://doi.org/10.1016/S0968-0004(97)01132-8

[35] Huang, C.H. and Peng, J. (2005) Evolutionary Conservation and Diversification of Rh Family Genes and Proteins. *Proceedings of the National Academy of Sciences*, **102**, 15512-15517. https://doi.org/10.1073/pnas.0507886102

[36] Nakhoul, N.L. and Hamm, L.L. (2004) Non-Erythroid Rh Glycoproteins: A Putative New Family of Mammalian Ammonium Transporters. *Pflugers Archiv—European Journal of Physiology*, **447**, 807-812. https://doi.org/10.1007/s00424-003-1142-8

[37] Soupene, E., King, N., Field, E., Liu, P., Niyogi, K.K., Huang, C.H., *et al.* (2002) Rhesus Expression in a Green Alga Is Regulated by CO_2. *Proceedings of the National Academy of Sciences*, **99**, 7769-7773. https://doi.org/10.1073/pnas.112225599

[38] Michele, R.D., Loque, D., Lalonde, S. and Frommer, W.B. (2012) Ammonium and Urea Transporter Inventory of the Selaginella and Physcomitrella Genomes. *Front Plant Science*, **3**, 62. https://doi.org/10.3389/fpls.2012.00062

[39] Suzuki, A., Komata, H., Iwashita, S., Seto, S., Ikeya, H., Tabata, M., *et al.* (2017) Evolution of the RH Gene Family in Vertebrates Revealed by Brown Hagfish (*Eptatretus atami*) Genome Sequences. *Molecular Phylogenetics Evolution*, **107**, 1-9. https://doi.org/10.1016/j.ympev.2016.10.004

[40] Aguera, E., Cabello, P. and Haba, P. (2010) Induction of Leaf Senescence by Low Nitrogen Nutrition in Sunflower (*Helianthus annuus*) Plants. *Physiologia Planta-*

rum, **138**, 256-267. https://doi.org/10.1111/j.1399-3054.2009.01336.x

[41] Meng, S., Peng, J.S., He, Y.N., Zhang, G.B., Yi, H.Y., Fu, Y.L., *et al.* (2016) *Arabidopsis* NRT1.5 Mediates the Suppression of Nitrate Starvation-Induced Leaf Senescence by Modulating Foliar Potassium Level. *Molecular Plant*, **9**, 461-470. https://doi.org/10.1016/j.molp.2015.12.015

[42] Till, I., Anna, M.Z., Marion, K. and Peter, D. (2006) A Salvage Pathway for Phytol Metabolism in *Arabidopsis*. *The Journal of Biological Chemistry*, **281**, 2470-2477 https://doi.org/10.1074/jbc.M509222200

[43] Gomez, F., Carrión, C., Costa, M., Desel, C., Kieselbach, T., Funk, C., *et al.* (2019) Extra-Plastidial Degradation of Chlorophyll and Photosystem I in Tobacco Leaves Involving "Senescence-Associated Vacuoles". *The Plant Journal*, **99**, 465-477. https://doi.org/10.1111/tpj.14337

[44] Edward, H. and Amasino, R.M. (2001) Nutrients Mobilized from Leaves of *Arabidopsis thaliana* during Leaf Senescence. *Journal of Plant Physiology*, **158**, 1317-1323. https://doi.org/10.1078/0176-1617-00608

[45] Reed, R. (1990) Solute Accumulation and Osmotic Adjustment. Cambridge University, New York.

[46] Xu, G., Fan, X. and Miller, A.J. (2012) Plant Nitrogen Assimilation and Use Efficiency. *Annual Review of Plant Biology*, **63**, 153-182. https://doi.org/10.1146/annurev-arplant-042811-105532

[47] Imamura, S., Terashita, M., Ohnuma, M., Maruyama, S., Minoda, A., Weber, A.P.M., *et al.* (2010) Nitrate Assimilatory Genes and Their Transcriptional Regulation in a Unicellular Red Alga *Cyanidioschyzon merolae*: Genetic Evidence for Nitrite Reduction by a Sulfite Reductase-Like Enzyme. *Plant and Cell Physiology*, **51**, 707-717. https://doi.org/10.1093/pcp/pcq043

[48] Gregersen, P.L., Holm, P.B. and Krupinska, K. (2008) Leaf Senescence and Nutrient Remobilisation in Barley and Wheat. *Plant Biology*, **10**, 37-49. https://doi.org/10.1111/j.1438-8677.2008.00114.x

[49] Diaz, C., Lemaitre, T., Christ, A., Azzopardi, M., Kato, Y., Sato, F., *et al.* (2008) Nitrogen Recycling and Remobilization Are Differentially Controlled by Leaf Senescence and Development Stage in Arabidopsis under Low Nitrogen Nutrition. *Plant Physiology*, **147**, 1437-1449. https://doi.org/10.1104/pp.108.119040

[50] Peng, J. and Huang, C.H. (2006) Rh Proteins vs Amt Proteins: An Organismal and Phylogenetic Perspective on CO_2 and NH_3 Gas Channels. *Transfusion Clinique et Biologique*, **13**, 85-94. https://doi.org/10.1016/j.tracli.2006.02.006

[51] Soupene, E., Inwood, W. and Kustu, S. (2004) Lack of the Rhesus Protein Rh1 Impairs Growth of the Green Alga *Chlamydomonas reinhardtii* at High CO_2. *Proceedings of the National Academy of Sciences*, **101**, 7787-7792. https://doi.org/10.1073/pnas.0401809101

Table S1. Chemical compositions of ESS_2.

Chemical composition	ESS_2[a]
HEPES (g/L)	10
$NaNO_3$ (g/L)	5
Na_2-glycerophosphate (mg/L)	800
Fe-EDTA·$3H_2O$ (mg/L)	300
KI (mg/L)	2
Na_2-EDTA (mg/L)	400
$FeCl_3$·$6H_2O$ (mg/L)	19.36
H_3BO_3 (mg/L)	456
$MnCl_2$·$4H_2O$ (mg/L)	0.576
$ZnCl_2$ (mg/L)	41.6
$CoCl_2$·$6H_2O$ (mg/L)	1.616
Vitamin B12 (mg/L)	0.1
Biotin (mg/L)	0.1
Thiamine-HCL (mg/L)	10
Nicotinic acid (mg/L)	10
Ca-pantothenate (mg/L)	10
p-aminobenzoic acid (mg/L)	1
Inositol (mg/L)	100
Thymine (mg/L)	10

[a]Final concentration of ESS_2 in sterilized artificial seawater was 1%.

Table S2. Land plant and algal AMTs and Rhs used for the phylogenetic analysis.

Species	Gene symbol/Annotation	Accession No.	Division	AAs
Aquilegia coerulea		PIA32185.1	Streptophyta	468
Aquilegia coerulea		PIA65513.1	Streptophyta	475
Aquilegia coerulea		PIA59506.1	Streptophyta	489
Aquilegia coerulea		PIA35542.1	Streptophyta	479
Aquilegia coerulea		PIA31609.1	Streptophyta	477
Aquilegia coerulea		PIA31140.1	Streptophyta	485
Aquilegia coerulea		PIA45105.1	Streptophyta	481
Arabidopsis thaliana	*AMT*1.1	AEE83287.1	Streptophyta	501
Arabidopsis thaliana	*AMT*1.2	AAD38253.1	Streptophyta	514
Arabidopsis thaliana	*AMT*1.3	AEE76886.1	Streptophyta	498
Arabidopsis thaliana	*AMT*1.4	AEE85527.1	Streptophyta	504
Arabidopsis thaliana	*AMT*1.5	AEE76885.1	Streptophyta	496
Arabidopsis thaliana	*AMT*2	AEC09519.1	Streptophyta	475
Chlamydomonas reinhardtii	ammonium transporter	XP_001702082.1	Chlorophyta	432
Chlamydomonas reinhardtii	ammonium transporter	XP_001692671.1	Chlorophyta	542
Chlamydomonas reinhardtii	ammonium transporter	XP_001693464.1	Chlorophyta	499
Chlamydomonas reinhardtii	ammonium transporter	XP_001697504.1	Chlorophyta	539
Chlamydomonas reinhardtii	ammonium transporter	AAS90602.1	Chlorophyta	579
Chlamydomonas reinhardtii	ammonium transporter	XP_001695208.1	Chlorophyta	610
Chlamydomonas reinhardtii	ammonium transporter	XP_001692923.1	Chlorophyta	481
Chlamydomonas reinhardtii	*AMT*1.2	AAM94623.2	Chlorophyta	542
Chlamydomonas reinhardtii	*Rh*1	XP_001695464.1	Chlorophyta	574
Chlamydomonas reinhardtii	*Rh*2	AAM19664.1	Chlorophyta	638
Chondrus crispus	unnamed protein product	XP_005710198.1	Rhodophyta	458
Cyanidioschyzon merolae	ammonium transporter	XP_005536541.1	Rhodophyta	373
Cylindrotheca fusiformis	*AMT*1	AAV70489.1	Heterokontophyta	511
Cylindrotheca fusiformis	*AMT-like*	AAV70490.1	Heterokontophyta	511
Ectocarpus siliculosus	ammonium transporter	CBN77717.1	Heterokontophyta	494
Emiliania huxleyi	ammonium transporter	XP_005785348.1	Heterokontophyta	462
Galdieria sulphuraria	ammonium transporter	EME32138.1	Rhodophyta	502
Galdieria sulphuraria	ammonium transporter	EME30100.1	Rhodophyta	604
Homo sapiens	*Rh* (*CE*)	NP_065231.3	Mammalia	417
Homo sapiens	*Rh* (*D*)	NP_001269800.1	Mammalia	493
Phaeodactylum tricornutum	ammonium transporter	XP_002176480.1	Heterokontophyta	540
Phalaenopsis equestris	ammonium transporter 1 member 2-like	XP_020575103.1	Magnoliophyta	514
Physcomitrella patens	ammonium transporter	XP_001758600.1	Bryophyta	504
Physcomitrella patens	ammonium transporter	XP_001758599.1	Bryophyta	503
Physcomitrella patens	ammonium transporter	PNR26034.1	Bryophyta	440
Physcomitrella patens	ammonium transporter	XP_001758603.1	Bryophyta	505

Continued

Physcomitrella patens	ammonium transporter	XP_001786055.1	Bryophyta	495
Physcomitrella patens	ammonium transporter	XP_001785500.1	Bryophyta	505
Physcomitrella patens	ammonium transporter	XP_001758611.1	Bryophyta	511
Physcomitrella patens	ammonium transporter	XP_001778521.1	Streptophyta	563
Physcomitrella patens	ammonium transporter	XP_001770054.1	Streptophyta	498
Physcomitrella patens	ammonium transporter	XP_001762803.1	Streptophyta	475
Physcomitrella patens	ammonium transporter	XP_001754238.1	Streptophyta	493
Physcomitrella patens	ammonium transporter	XP_001752514.1	Streptophyta	490
Physcomitrella patens	ammonium transporter	XP_001781204.1	Streptophyta	495
Physcomitrella patens	ammonium transporter	XP_001754816.1	Streptophyta	494
Porphyra purpurea	Contig05572		Rhodophyta	455
Porphyra purpurea	Contig8812		Rhodophyta	487
Porphyra purpurea	Contig05687		Rhodophyta	489
Porphyra purpurea	Contig2135		Rhodophyta	485
Porphyra umbilicalis	Pum0027s0002.1 (*AMT*2.2)	OSX80976.1	Rhodophyta	411
Porphyra umbilicalis	Pum0165s0019.1 (*AMT*2.1)	OSX69292.1	Rhodophyta	644
Porphyra umbilicalis	Pum0463s0020.1 (*AMT*1.2)	OSX72158.1	Rhodophyta	545
Porphyra umbilicalis	Pum0126s0003.1 (*AMT*1.4)	OSX77964.1	Rhodophyta	480
Porphyra umbilicalis	Pum0165s0019.1 (*AMT*1.1)	OSX77025.1	Rhodophyta	485
Porphyra umbilicalis	Pum1775s0001.1 (*AMT*1.3)	OSX69172.1	Rhodophyta	428
Porphyra umbilicalis	Pum0022s0083.1 (*AMT*3)	OSX81363.1	Rhodophyta	616
Porphyridium purpureum	contig3836.1		Rhodophyta	562
Porphyridium purpureum	contig2277.5		Rhodophyta	517
Porphyridium purpureum	contig2333.1		Rhodophyta	492
Porphyridium purpureum	contig2015.11		Rhodophyta	444
Pyropia yezoensis	*AMT*1	BAV55983.1	Rhodophyta	483
Pyropia yezoensis	*AMT*1.2	MK537329	Rhodophyta	484
Pyropia yezoensis	*AMT*1.3	MK537330	Rhodophyta	654
Pyropia yezoensis	*AMT*1.4	MK537331	Rhodophyta	589
Pyropia yezoensis	*AMT*1.5	MK537332	Rhodophyta	616
Pyropia yezoensis	*AMT*1.6	MK537333	Rhodophyta	690
Pyropia yezoensis	*Rh*	MK537334	Rhodophyta	522
Sus scrofa	Rh protein	BAB84562.1	Mammalia	423
Volvox carteri f. nagariensis		EFJ48363.1	Chlorophyta	426
Volvox carteri f. nagariensis		EFJ41931.1	Chlorophyta	518
Volvox carteri f. nagariensis		EFJ47696.1	Chlorophyta	496
Volvox carteri f. nagariensis		EFJ41931.1	Chlorophyta	518
Volvox carteri f. nagariensis		EFJ40601.1	Chlorophyta	570
Volvox carteri f. nagariensis		EFJ43712.1	Chlorophyta	639
Volvox carteri f. nagariensis		EFJ47052.1	Chlorophyta	463
Volvox carteri f. nagariensis		EFJ51468.1	Chlorophyta	453

Table S3. Primer sequences used for quantitative PCR analyses.

Primer name	Sequence (5'-3')	Annealing temperature (˚C)	Product size (bp)
Q-Py18S-F	CGACCGTTTACTGTGAAG	58	160
Q-Py18S-R	GACAATGAAATACGAATGCC		
Q-PyAMT1-F	TGTGGTTTGGGTGGTACGG	60	169
Q-PyAMT1-R	GCAGCTTGATGACAATGAGGG		
Q-PyAMT1.2-F	GTGGCCGAGGAAGGGATT	59	132
Q-PyAMT1.2-R	AGCGTGCGGACAAAGAAC		
Q-PyAMT1.3-F	TCCAATCCTTGCTTTTCA	60	98
Q-PyAMT1.3-R	GTTCCCGCTTGCTCCATA		
Q-PyAMT1.4-F	GGGCGGGTTTATCTTGTG	58	162
Q-PyAMT1.4-R	GTCTGCTGGACGGTGAGG		
Q-PyAMT1.5-F	CCGAGTATGGGTGGTTGG	60	152
Q-PyAMT1.5-R	GGTGGGTAGGCGGTGAAG		
Q-PyAMT1.6-F	GCGGGCATGGAAGGACAG	57	145
Q-PyAMT1.6-R	AAGGCGGGGAAGGAGGGA		
Q-PyRh-F	AAGCGAGAAGACGGAGCA	62	194
Q-PyRh-R	TGGAAGACATTCAGAACG		

Table S4. Physical and chemical characteristics of PyAMTs and *PyRh*.

Name	Amino acids numbers	Molecular weight	Total number of atoms	Isoelectric point (pI)	Grand average of hydropathicity (GRAVY)	Ammonium transporter domain location[a]	Accession number
PyAMT1	483	50.98	7164	4.8	0.637	40 - 449	BAV55983.1
PyAMT1.2	484	51.2	7202	4.79	0.555	38 - 448	MK537329
PyAMT1.3	654	67.8	9576	6.16	0.518	75 - 505	MK537330
PyAMT1.4	589	58.67	8227	5.98	0.543	53 - 486	MK537331
PyAMT1.5	616	63.68	8934	5.08	0.501	51 - 473	MK537332
PyAMT1.6	690	72.06	10149	9.21	0.39	52 - 474	MK537333
PyRh	522	53.78	7540	5.5	0.543	30 - 431	MK537334

[a]The number indicating positions of ammonium transporter domains is based on assignment of the start methionine residue as 1 in PyAMTs and *PyRh*.

Table S5. Locations of transmembrane (TM) helices in PyAMT1s and *PyRh*[a].

TM helices	PyAMT1[b]	PyAMT1.2	PyAMT1.3	PyAMT1.4	PyAMT1.5	PyAMT1.6	*PyRh*
1	41 - 63	40 - 62	7 - 29	5 - 27	29 - 47	34 - 48	21 - 43
2	76 - 98	75 - 97	77 - 99	52 - 74	51 - 73	52 - 74	63 - 85
3	118 - 140	117 - 139	120 - 142	86 - 108	85 - 107	86 - 108	92 - 114
4	147 - 169	146 - 168	157 - 176	132 - 154	140 - 162	140 - 162	129 - 151
5	184 - 206	183 - 205	183 - 204	159 - 181	167 - 189	169 - 191	158 - 180
6	218 - 240	217 - 239	224 - 246	201 - 223	215 - 226	214 - 236	190 - 207
7	262 - 284	261 - 283	267 - 289	244 - 263	255 - 277	249 - 271	227 - 244
8	296 - 318	290 - 309	324 - 343	306 - 328	290 - 312	291 - 313	259 - 281
9	322 - 344	319 - 341	350 - 372	341 - 374	327 - 349	325 - 347	294 - 311
10	351 - 373	346 - 368	377 - 394	389 - 411	370 - 392	375 - 397	315 - 337
11	402 - 424	401 - 423	452 - 474	414 - 430	424 - 446	421 - 443	349 - 371
12							399 - 412

[a]The number indicating positions of TM helices is based on assignment of the start methionine residue as 1 in PyAMTs and *PyRh*.